Scientific Reports

https://doi.org/10.1038/s41598-026-60833-y

Article in Press

Hybrid steel and carbon fiber reinforcement enhances mechanical performance and sustainability of cementitious composites

Received: 22 April 2026

Accepted: 30 June 2026

Published online: 02 July 2026

Cite this article as: Ozturk M. & Arpaci S.S. Hybrid steel and carbon fiber reinforcement enhances mechanical performance and sustainability of cementitious composites. *Sci Rep* (2026). https://doi.org/10.1038/s41598-026-60833-y

Murat Ozturk & Sebnem Sevil Arpaci

We are providing an unedited version of this manuscript to give early access to its findings. Before final publication, the manuscript will undergo further editing. Please note there may be errors present which affect the content, and all legal disclaimers apply.

If this paper is publishing under a Transparent Peer Review model then Peer Review reports will publish with the final article.

ARTICLE IN PRESS

© The Author(s) 2026. **Open Access** This article is licensed under a Creative Commons Attribution-NonCommercial-NoDerivatives 4.0 International License, which permits any non-commercial use, sharing, distribution and reproduction in any medium or format, as long as you give appropriate credit to the original author(s) and the source, provide a link to the Creative Commons licence, and indicate if you modified the licensed material. You do not have permission under this licence to share adapted material derived from this article or parts of it. The images or other third party material in this article are included in the article's Creative Commons licence, unless indicated otherwise in a credit line to the material. If material is not included in the article's Creative Commons licence and your intended use is not permitted by statutory regulation or exceeds the permitted use, you will need to obtain permission directly from the copyright holder. To view a copy of this licence, visit http://creativecommons.org/licenses/by-nc-nd/4.0/.

ARTICLE IN PRESS

Hybrid Steel and Carbon Fiber Reinforcement Enhances Mechanical Performance and Sustainability of Cementitious Composites

Murat OZTURK[1]* and Sebnem Sevil ARPACI[2]

[1] Smart Materials Laboratory, Bursa Uludag University, Engineering Faculty, Civil Engineering, Bursa 16059, Türkiye
[2] Bursa Technical University, Faculty of Forestry, Forest Industry Engineering, Bursa 16310, Türkiye
* Corresponding author. ORCID ID: 0000-0003-3389-4883; Email: muratozturk@uludag.edu.tr

Abstract

This study investigates the synergistic effects of hybrid steel fiber (SF) and carbon fiber (CF) reinforcement on the mechanical, microstructural, and sustainability profiles of cementitious composites. While fiber-reinforced mortars are known for enhanced ductility, the multi-scale interaction between macro-scale SF and micro-scale CF remains under-explored in the context of simultaneous environmental and economic optimization. Experimental results demonstrate that the hybrid integration of 0.37% SF and 0.10% CF achieves a superior flexural-to-compressive strength ratio, attributed to a hierarchical crack-arrest mechanism. Microstructural analysis via Mercury Intrusion Porosimetry (MIP) and Scanning Electron Microscopy (SEM) confirms that CF acts as a pore-refiner, densifying the interfacial transition zone (ITZ). Furthermore, a cradle-to-gate Life Cycle Assessment (LCA) and cost-efficiency analysis were integrated into a novel 'Performance Index' (PI) to resolve the trade-offs between technical performance and sustainability. The findings reveal that optimized hybrid systems provide a more sustainable alternative to mono-fiber systems, offering a balanced solution for high-performance and eco-friendly construction materials.

Keywords: Steel fiber; Carbon fiber; hybrid; LCA; Cost

1. Introduction

Cementitious composites have become an indispensable component of modern infrastructure due to their wide availability, ease of processing, high compressive strength, and long-term durability [1]. When the built environment is observed, it can easily be recognized that a significant portion of structural elements has been constructed using cement-based composites. Despite their advantageous compressive performance, these materials are inherently brittle and exhibit relatively low resistance to tensile stresses [2].

ARTICLE IN PRESS

Consequently, extensive research has been conducted for decades to improve the tensile behavior and crack resistance of cementitious materials [3–6].

One of the most widely adopted approaches for enhancing tensile performance is the use of steel reinforcement embedded within concrete, which forms the basis of reinforced concrete structures [7–9]. In this system, the tensile stresses that develop under external loading are largely carried by the reinforcing steel bars, thereby increasing the overall structural capacity and ductility.

Another widely implemented method for improving tensile performance is the incorporation of fibers into the cementitious matrix. Randomly distributed fibers within the composite act as crack-bridging elements and contribute to the transfer of tensile stresses across microcracks [10,11]. As a result, the tensile strength, toughness, and post-cracking behavior of the composite can be significantly improved [12–17]. The overall performance of fiber-reinforced cementitious composites is influenced by several parameters, including fiber type, geometry, aspect ratio, orientation, and volume fraction [18–20].

Various types of fibers have been utilized in cementitious composites. Synthetic fibers such as polypropylene fibers, carbon fibers, aramid fibers, acrylic fibers, and polyvinyl alcohol fibers have been widely investigated [21–23]. In addition, natural fibers including jute, wood, and hemp have also attracted attention due to their sustainability potential [24,25]. Metallic fibers, particularly steel and aluminum fibers, have also been employed to enhance the mechanical performance of cement-based materials [26–28]. Among these alternatives, steel fibers and carbon fibers have received considerable attention in the development of high-performance composites. Steel fibers provide high elastic modulus, significant tensile strength, and good compatibility with the cement matrix [29], while carbon fibers offer extremely high tensile strength, excellent chemical stability, and superior durability [30]. The continuous development of fiber-reinforced composites has been driven not only by the pursuit of enhanced mechanical performance but also by increasing demands for material efficiency and sustainability in engineering applications [31–33].

Several studies in the literature have indicated that hybrid fiber systems may improve parameters such as flexural strength, toughness, and energy absorption capacity [34–38]. However, compared with studies focusing on the individual use of fibers, research investigating hybrid fiber combinations remains relatively limited. Therefore, further studies are required in order to better understand the interaction mechanisms between different fiber types within cementitious matrices.

ARTICLE IN PRESS

The fundamental challenge in optimizing fiber-reinforced cementitious composites lies in the disparate scales at which different fiber types operate. While macro-steel fibers (SF) are widely recognized for their ability to bridge significant cracks and provide post-peak ductility, they are often less effective during the micro-crack initiation stage. Conversely, micro-scale carbon fibers (CF) exhibit a high elastic modulus and surface area, allowing them to intercept micro-cracks before they coalesce into macro-scale failures. However, the literature remains fragmented regarding the synergistic integration of these two materials, particularly concerning the balance between mechanical superiority, environmental GWP (Global Warming Potential), and cost-efficiency. This study addresses this gap by proposing a hierarchical crack-arrest mechanism where SF and CF operate across multiple scales. To validate this mechanism, a comprehensive experimental program is conducted, encompassing compressive and flexural strength tests to evaluate mechanical performance, alongside Mercury Intrusion Porosimetry (MIP) and Scanning Electron Microscopy (SEM) to characterize microstructural evolution and pore refinement. Furthermore, a cradle-to-gate Life Cycle Assessment (LCA) and cost-efficiency analysis are integrated through a novel Performance Index (PI) to identify the optimal hybrid fiber equilibrium. Through this integrated approach, the research provides a robust pathway for developing next-generation, eco-efficient, and high-performance cementitious materials.

2. Materials and method

2.1 Raw Materials

The mortar mixtures investigated in this study consist of ordinary Portland cement, calcareous fine aggregate, mixing water, SF, and CF. Ordinary Portland cement (CEM I 42.5R) supplied by Bursa Cement (Bursa, Türkiye) is used as the binder material. The cement has a specific gravity of 3.10.

Crushed calcareous aggregate with a maximum particle size of 4 mm is employed as the fine aggregate. The aggregate has a specific gravity of 2.65. Potable tap water is used during the preparation of all mortar mixtures.

Steel fibers with a diameter of 0.1 mm and a length of 10 mm are incorporated into the mortar matrix. These fibers have a tensile strength of approximately 2500 MPa and are commercially produced by Dramix (Türkiye). In addition to steel fibers, short carbon fibers are utilized as a secondary reinforcement. The carbon fibers have an approximate diameter of 7 μm, a length of 10 mm, and a tensile strength of about 4200 MPa. These fibers possess a kidney-beam type cross-section and are supplied as Aksaca™ 24K A-42 filament yarn by DowAksa (Türkiye).

2.2 Mixture Proportions

ARTICLE IN PRESS

In order to isolate the influence of fiber reinforcement, the proportions of cement, aggregate, and water are kept constant for all mixtures. The binder, aggregate, and water ratio is maintained at 1:2.75:0.485 by mass. The experimental program focuses on the variation of fiber content.

Steel fibers are incorporated at volumetric ratios of 0.50%, 0.75%, and 1.00%, while carbon fibers are added at 0.10%, 0.20%, and 0.30% by volume of the composite. The fiber dosages are selected based on a parametric experimental design spanning a range from low to workability-limiting fiber contents. The upper bounds are constrained by fresh mortar workability: beyond 1.00% SF and 0.30% CF, severe fiber balling and workability loss are observed, making uniform specimen casting impractical. Both single-fiber systems and hybrid fiber combinations are evaluated in order to examine potential synergistic effects between the two fiber types. The detailed mixture compositions are presented in Table 1.

Table 1. Mix design and experimental matrix of steel and carbon fiber reinforced mortars (per 1 m^3)

Mix ID	Aggregate (kg)	Cement (kg)	Water (kg)	SF (kg)	CF (kg)	SF (vol%)	CF (Vol%)
0SF-0CF	1490	542	263	0	0	0	0
0.50SF-0CF	1490	542	263	35.50	0	0.50	0
0.75SF-0CF	1490	542	263	53.25	0	0.75	0
1.00SF-0CF	1490	542	263	71.00	0	1.00	0
0SF-0.10CF	1490	542	263	0	1.81	0	0.10
0SF-0.20CF	1490	542	263	0	3.62	0	0.20
0SF-0.30CF	1490	542	263	0	5.43	0	0.30
0.25SF-0.05CF	1490	542	263	17.75	0.90	0.25	0.05
0.37SF-0.10CF	1490	542	263	26.62	1.81	0.375	0.10
0.50SF-0.15CF	1490	542	263	35.5	2.71	0.50	0.15

ARTICLE IN PRESS

2.3 Specimen Preparation and Curing

ARTICLE IN PRESS

All mixtures are prepared using a mechanical mixer. Initially, the dry constituents, including cement, fine aggregate, and fibers, are blended to achieve a uniform distribution of the fibers within the mixture. Subsequently, the mixing water is gradually introduced while mixing continues until a homogeneous mortar with adequate workability is obtained.

The fresh mortar is cast into lubricated steel molds. Prismatic specimens measuring 40 × 40 × 160 mm^3 are produced for flexural strength testing, while cubic specimens with dimensions of 50 × 50 × 50 mm^3 are prepared for compressive strength measurements.

After casting, the specimens are kept in the molds for 24 hours under laboratory conditions. Following demolding, the samples are submerged in water and cured at ambient temperature until the testing age of 28 days.

2.4 Mechanical Testing

Flexural strength is determined using a three-point bending test on 40 × 40 × 160 mm^3 prismatic specimens in accordance with ASTM C348. Load is applied at the mid-span until failure occurs. The reported flexural strength corresponds to the average of at least three specimens for each mixture. Compressive strength is measured on 50 × 50 × 50 mm^3 cubic specimens in accordance with ASTM C109. Six specimens are tested for each mixture, and the average compressive strength value is reported.

2.5 Microstructural and Pore Structure Analysis

The pore characteristics of hardened mortar samples are investigated by MIP using a PoreMaster 33 instrument. Approximately 2 g of fragments are collected from the internal region of specimens after compressive strength testing. Prior to the analysis, the samples are dried in a vacuum oven at 60 °C for 24 hours.

Mercury intrusion is performed through successive low-pressure and high-pressure stages, with the maximum applied pressure reaching approximately 33,000 psi. The pore size distribution and cumulative intrusion volume are calculated using the Washburn equation.

Microstructural observations are conducted using a ZEISS EVO 40 scanning electron microscope. Before SEM imaging, the samples are vacuum-dried and coated with a thin layer of gold in order to improve electrical conductivity. SEM micrographs are obtained at various magnifications to evaluate the morphology of the mortar matrix and the interaction between fibers and the cementitious matrix.

2.6. Life Cycle Assessment (LCA) Methodology

ARTICLE IN PRESS

A "cradle-to-gate" Life Cycle Assessment (LCA) was conducted to evaluate the environmental impacts of incorporating steel and carbon fibers into the mortar mixtures. The functional unit was defined as 1 m^3 of produced mortar, based on the mix proportions detailed in Table 1. The system boundary encompassed raw material extraction, manufacturing, and mortar production.

The LCA was modeled using OpenLCA software with background inventory data sourced from the ELCD 3.2 (European Reference Life Cycle Database), which reflects European average conditions. While the scope covered raw material extraction and manufacturing stages, the transport of raw materials to the production plant, as well as end-of-life and use-phase impacts, were excluded from the system boundary due to the lack of site-specific data. This boundary selection is consistent with similar cradle-to-gate LCA studies on cementitious composites in the literature. Furthermore, a mass-based allocation method was applied where co-production was involved. Table 2 presents the background inventory data, including approximate unit material costs (USD/kg), approximate GWP emission factors (kg CO_2/kg) and the corresponding ELCD 3.2 dataset identifiers for all mortar constituents. Additionally, the final cradle-to-gate environmental impact assessment results for all studied mortar mixtures are detailed in Table 3.

Table 2. Life cycle inventory (LCI) source data, dataset identifiers, and approximate unit parameters for mortar constituents.

Constituent	**ELCD 3.2 / Source Dataset Identifier**	**Approx.Unit Cost(USD/kg)***	**Approx. GWP Emission Factor (kg CO_2/kg)**
Carbon Fiber	carbon fiber	*15.00*	*24.50*
Crushed Stone	Crushed stone 16/32, production mix, at plant, open pit mining	*0.02*	*0.005*
Portland Cement	Portland cement (CEM I), CEMBUREAU production mix, at plant	*0.12*	*0.82*

ARTICLE IN PRESS

Constituent	ELCD 3.2 / Source Dataset Identifier	Approx.Unit Cost(USD/kg)*	Approx. GWP Emission Factor (kg CO_2/kg)
Silica Fume	Silica fume, co-product of ferrosilicon production, at plant	*0.40*	*0.025*
Water	Tap water, from surface water, at user	*0.001*	*0.0003*

** Material costs are approximate values based on global market averages for the years 2024–2025.*

Table 3: Environmental impact assessment results of the studied mortar mixtures based on ReCiPe 2016 Midpoint (H) method.

Mix Name	Global Warming (kg CO_2)	Fine Particulate Matter(kg PM2.5)	Fossil Resource Scarcity (kg oil)	Terrestrial Acidification (kg SO_2)	Water Consumption (m^3)
mix_0SF-0CF	2,387	2.59	510	8.85	-2.82
mix_0SF-0.10CF	2,441	2.65	510	9.07	-2.82
mix_0sf0.2cf	2,496	2.71	510	9.28	-2.82
mix_0sf0.3cf	2,550	2.78	510	9.50	-2.82
mix_0.5sf0cf	2,431	2.62	520	8.95	-2.81
mix_0.75sf0cf	2,453	2.64	526	9.00	-2.81

ARTICLE IN PRESS

ARTICLE IN PRESS

Mix Name	Global Warming (kg CO_2)	Fine Particulate Matter(kg PM2.5)	Fossil Resource Scarcity (kg oil)	Terrestrial Acidification (kg SO_2)	Water Consumption (m^3)
mix_1sf0cf	2,475	2.66	531	9.06	-2.80
mix_0.25SF-0.05CF	2,436	2.64	515	9.01	-2.82
mix_0.37SF-0.10CF	2,474	2.68	518	9.14	-2.81
mix_0.50SF-0.15CF	2,512	2.72	520	9.28	-2.81

ARTICLE IN PRESS

2.7. Cost Estimation Analysis

A cost analysis was conducted to evaluate the economic viability of the designed mixtures. First, the total material cost (C_{total}) of each mixture was calculated using the unit prices of the raw materials (cement, aggregate, water, steel fibers, and carbon fibers). These prices were obtained from the Alibaba global wholesale platform and recorded in US Dollars (USD).

Two indices, cost per unit compressive strength (CP_{comp}) and cost per unit flexural strength (CP_{flex}) were calculated using the following equations:

$$CP_{comp} = \frac{C_{total}}{f_c} \quad (1)$$

$$CP_{flex} = \frac{C_{total}}{f_r} \quad (2)$$

where (C_{total}) is the total material cost of the mixture, f_c is the 28-day compressive strength (MPa), and f_r is the 28-day flexural strength (MPa). A lower index value indicates a more cost-effective mixture.

3. Results and discussion

3.1. Flexural tensile strength

ARTICLE IN PRESS

This section quantitatively investigates the multi-scale reinforcement effects of SF and CF combinations—both as mono-fillers and as hybrid systems—on the flexural performance of the composite matrix. As illustrated in Figure 1, when compared to the plain control specimen (5.6 MPa), the incorporation of fibers results in statistically significant enhancements across all experimental variants. In mono-fiber systems, a consistent and linear upward trend in flexural strength occurs as the fiber volume fraction increases. Specifically, increasing the SF volume fraction from 0.50% to 0.75% and 1.00% elevates the flexural strength to 7.1 MPa, 8.1 MPa, and 8.6 MPa, respectively, representing improvements ranging from 27% to 54% over the control. This confirms that the macro-scale crack-bridging mechanism provided by steel fibers correlates directly with the volume fraction, thereby effectively restricting macro-crack propagation [39].

The mono-addition of carbon fibers—even at notably low volume fractions of 0.10%, 0.20%, and 0.30%—yields significant flexural strengths of 7.5 MPa, 8.0 MPa, and 8.4 MPa. These results underscore the superior "reinforcement efficiency per unit volume" of carbon fibers compared to steel fibers. Due to their microscopic dimensions and high elastic modulus, carbon fibers minimize localized stress concentrations at crack tips, effectively arresting crack initiation at an early stage [40–42].

The individual contributions of SF and CF to crack control operate at distinct length scales. SF, with a diameter of 0.1 mm, a length of 10 mm, and a tensile strength of approximately 2500 MPa, primarily engages after matrix cracking, bridging macro-cracks and providing post-peak energy absorption through fiber pull-out and plastic deformation. This macro-scale bridging mechanism explains the continuous increase in flexural strength with increasing SF volume fraction. In contrast, CF, with a diameter of ~7 μm and a tensile strength of 4200 MPa, is mobilized at significantly lower strain levels. Due to their extremely fine dimensions, CF intercept micro-cracks at the initiation stage, distributing stress around crack tips and delaying crack coalescence into macro-fractures. The combination of these two mechanisms — micro-crack arrest by CF and macro-crack bridging by SF — constitutes the hierarchical crack-arrest mechanism responsible for the synergistic peak observed in the 0.37% SF + 0.10% CF hybrid mixture.

In hybrid fiber systems, the synergistic interaction between steel and carbon fibers peaks at the 0.37% SF + 0.10% CF combination, which achieves a flexural strength of 9.1 MPa—a remarkable 62.5% increase over the control. However, unlike the linear progression observed in mono-fiber systems, hybrid combinations exhibit a distinct decline in flexural strength once this optimum threshold is exceeded (e.g., in the 0.50% SF + 0.15% CF variant). While mono-fiber systems maintain a continuous growth trend, this decline in hybrid systems stems from "mechanical incompatibility" arising from the disparate geometric and mechanical properties of the macro- and micro-

ARTICLE IN PRESS

fibers. Exceeding the critical volume threshold induces severe fiber entanglement within the matrix, which impairs homogeneous distribution and compromises the structural integrity of the composite [43]. These findings demonstrate that the mechanical performance of hybrid-reinforced composites does not function strictly as a linear outcome of total fiber volume, but rather relies on a delicate balance of "optimum hybrid saturation," where macro and micro fibers exist in a configuration that precludes excessive geometric interference [44,45].

Error bars in Figures 1 and 2 represent standard deviation. The synergistic effect of the 0.37% SF + 0.10% CF hybrid system is evidenced by its flexural strength of 9.1 MPa, which exceeds the mono-CF result at the equivalent CF dosage (0.10% CF alone: 7.5 MPa) and is substantially higher than the lowest tested mono-SF result (0.50% SF: 7.1 MPa), with 0.37% SF being below the minimum mono-SF dosage evaluated. This difference clearly exceeds the error bar range shown in Figure 1, confirming a genuine hybrid performance enhancement beyond the individual contributions of each fiber type.

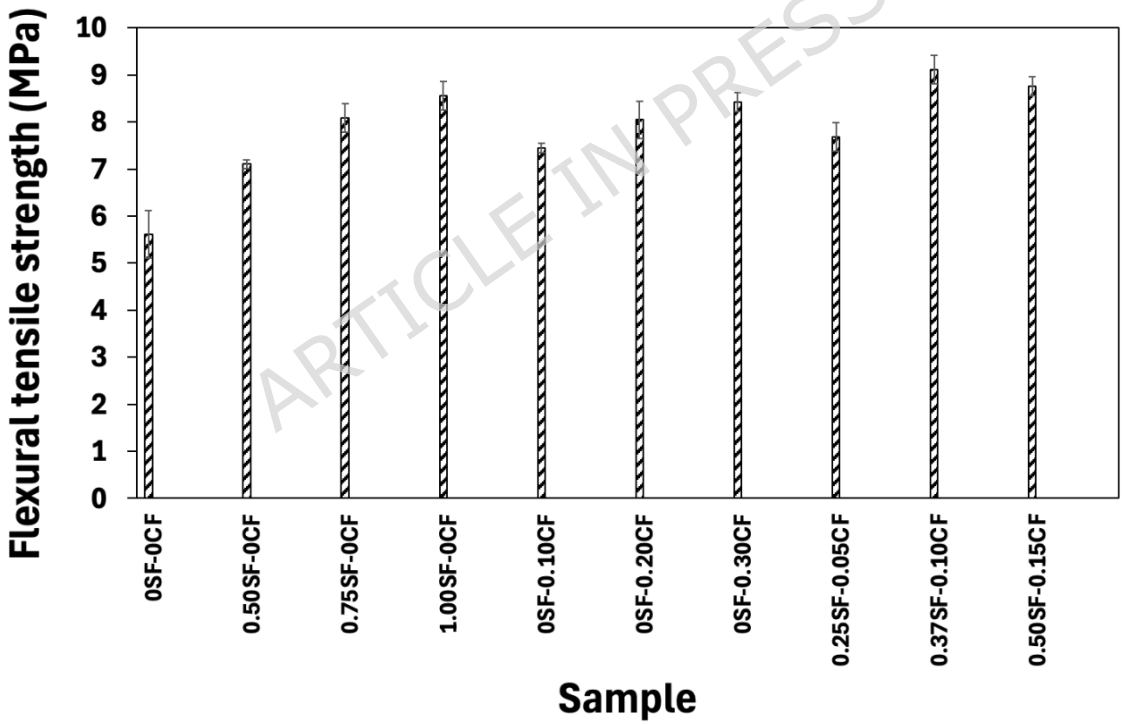


Figure 1. Flexural tensile strength of composite specimens reinforced with mono and hybrid steel and carbon fibers (Error bars represent standard deviation).

3.2. Compressive strength

ARTICLE IN PRESS

This section quantitatively evaluates the compressive strength behavior of the composite matrix under varying SF and CF reinforcement configurations. As illustrated in Figure 2, the inclusion of steel fibers leads to a consistent, albeit modest, improvement in compressive strength compared to the plain control specimen (64 MPa). Increasing the SF volume fraction to 0.50%, 0.75%, and 1.00% results in compressive strengths of approximately 69 MPa, 70 MPa, and 70 MPa, respectively. This trend indicates that while steel fibers effectively enhance ductility and post-crack energy absorption, their contribution to pure compressive strength remains relatively marginal once the matrix reaches an optimal packing density [46].

Conversely, the mono-addition of carbon fibers at 0.10%, 0.20%, and 0.30% results in compressive strengths of approximately 60 MPa, 62 MPa, and 58 MPa, respectively. These values reflect a slight decline compared to the control specimen. This reduction primarily stems from the inherent nature of the fiber-matrix interface and the specific volume occupied by the carbon fibers, which may introduce a slight reduction in the effective cross-sectional area of the cementitious matrix available to resist compressive loads [47].

In hybrid fiber systems (0.25% SF + 0.05% CF, 0.37% SF + 0.10% CF, and 0.50% SF + 0.15% CF), the compressive strength values fluctuate between approximately 57 MPa and 61 MPa. Unlike the synergistic effects observed in flexural performance, hybrid reinforcement does not yield a comparable improvement in compressive strength. The data suggests that as total fiber volume increases—particularly with the addition of micro-scale carbon fibers—the complexity of the internal fiber network leads to fiber entanglement. This phenomenon disrupts the optimal packing of the cement matrix, thereby slightly compromising the bulk compressive integrity. Consequently, while hybrid systems provide superior flexural capacity, they operate under a trade-off mechanism where the benefits of crack bridging are partially offset by a reduction in compressive density as the total fiber loading increases.

ARTICLE IN PRESS

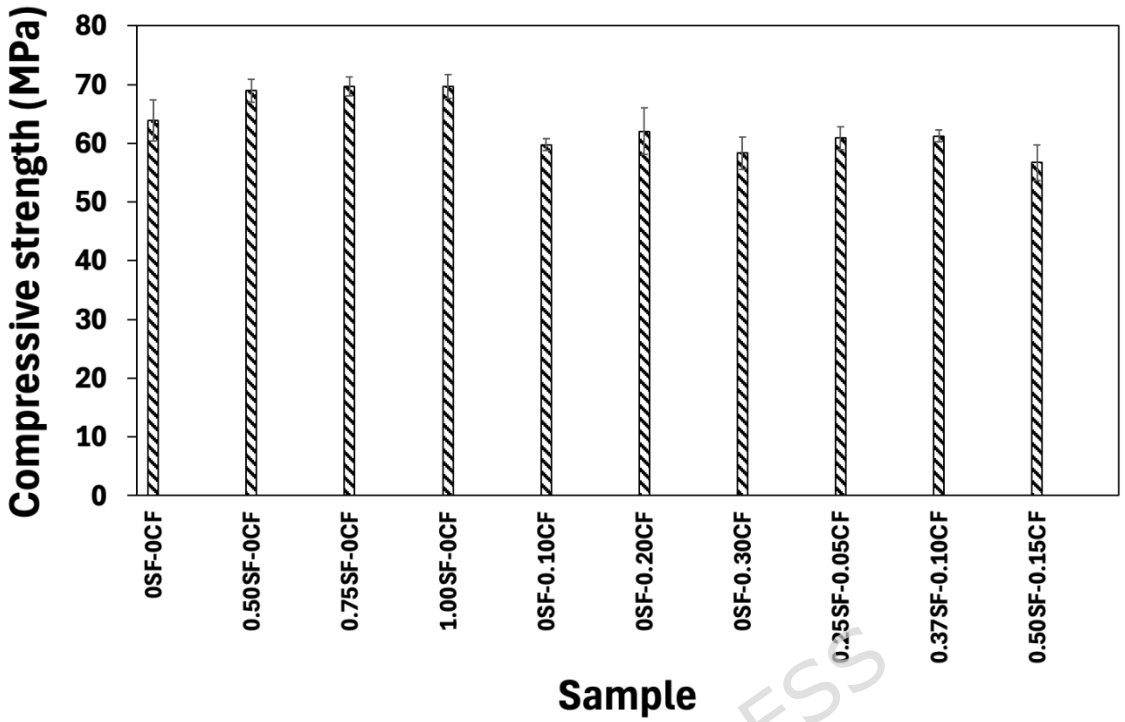


Figure 2. Compressive strength of composite specimens reinforced with mono and hybrid steel and carbon fibers (Error bars represent standard deviation).

3.3. Pore Structure Analysis (MIP)

The microstructural characteristics of cementitious composites serve as a fundamental determinant of their macro-scale mechanical behavior and long-term durability. The differential intrusion curves presented in Figure 3(a) illustrate that the incorporation of steel SF and CF significantly modifies the pore size distribution of the matrix. While the reference specimen (0SF-0CF) exhibits a high concentration of pores in the 50–100 nm range, the 1.00SF-0CF sample demonstrates the lowest cumulative intrusion (Figure 3(b)), indicating that a 1% volume fraction of steel fibers densifies the matrix by minimizing the total void volume. This structural densification correlates directly with an increase in compressive strength, as the reduction in total porosity limits stress concentration sites within the composite [48].

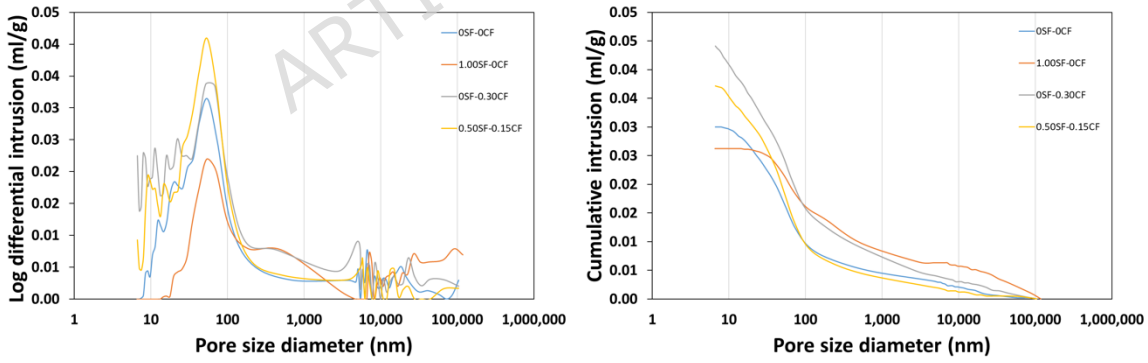
The pore structure of the hybrid fiber-reinforced sample (0.50SF-0.15CF) reveals a synergistic effect at the microscopic level. As shown in the volume fraction analysis (Figure 3(c)), approximately 70% of the pores in the hybrid system are concentrated within the 10–100 nm range, suggesting a significant pore refinement process. This refinement acts as the primary mechanism for enhanced flexural performance and toughness [49]; while macro-scale steel fibers bridge developing cracks to dissipate energy, the micro-scale carbon fibers bridge capillary voids and arrest the coalescence

ARTICLE IN PRESS

of micro-cracks at their inception. Importantly, the MIP data also provide microstructural support for the identification of 0.37% SF + 0.10% CF as the optimal hybrid mixture. At this dosage, the CF content is sufficient to initiate significant pore refinement — shifting a meaningful proportion of pores toward the 10–100 nm range — without inducing the agglomeration-related increase in total pore volume observed at higher CF contents. The 0.50% SF + 0.15% CF specimen, while exhibiting strong pore refinement, shows a slightly elevated total intrusion volume compared to the 0.37% SF + 0.10% CF specimen, attributable to the higher ITZ area generated by the greater CF content and potential localized fiber clustering. The 0.37% SF + 0.10% CF mixture therefore achieves the most favorable pore size distribution — minimizing macroporosity while maintaining adequate pore connectivity for hydration product growth — producing the microstructural conditions most conducive to the observed flexural performance peak.

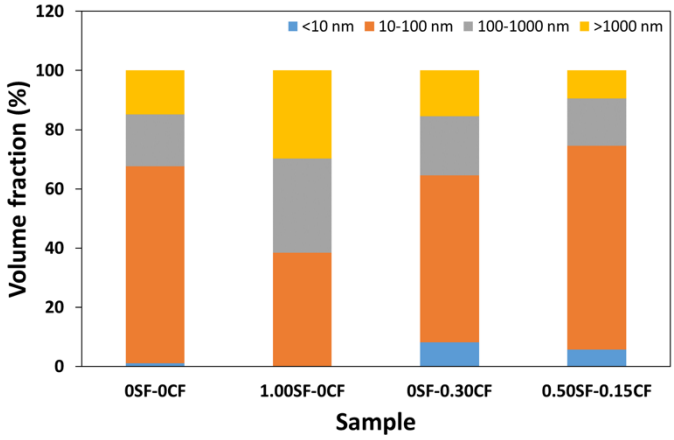
Interestingly, the 0SF-0.30CF sample exhibits the highest cumulative intrusion in Figure 3, which is attributed to the increased interfacial transition zones (ITZ) formed around the high-surface-area carbon fibers [50] or potential agglomeration [51]. This observation confirms that exceeding a certain dosage of micro-fibers can increase the total void volume, potentially leading to a slight reduction in compressive strength despite their benefits in crack control. However, the hybrid design (0.50SF-0.15CF) optimizes this trade-off; the pore-refining capability of carbon fibers complements the macro-scale reinforcement of steel fibers, resulting in an optimized microstructure that simultaneously provides high compressive strength and superior post-cracking ductility.

ARTICLE IN PRESS



(a) (b)

ARTICLE IN PRESS



(c)

Figure 3. MIP analysis of mono and hybrid fiber-reinforced composites: (a) differential pore volume, (b) cumulative intrusion, and (c) pore size classification.

3.4. SEM analysis

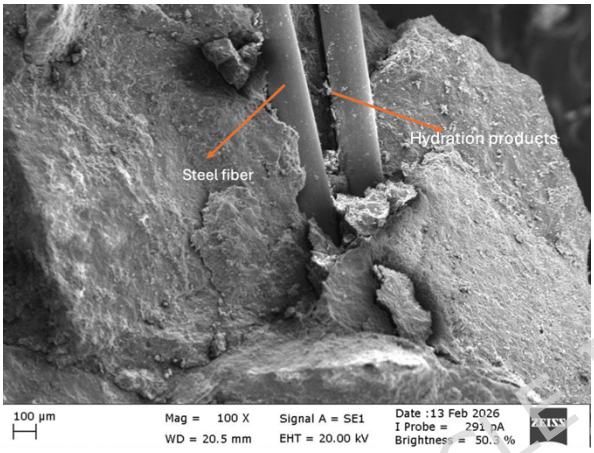
The microstructural evolution and the interfacial characteristics of the fiber-reinforced composites are examined through SEM, as presented in Figure 4 (a, b, and c). These micrographs provide direct visual evidence of the reinforcement mechanisms—mechanical interlocking, dispersion quality, and multi-scale synergy—that govern the macroscopic mechanical responses of the specimens.

Figure 4(a) illustrates the interfacial transition zone (ITZ) of the steel fiber (1.00SF-0CF) specimen. The image clearly depicts a robust mechanical interlocking between the coarser steel fiber and the surrounding cementitious matrix. The presence of hydration products adhering to the fiber surface suggests a strong interfacial bond [52], which is essential for the macro-scale crack-bridging mechanism discussed in the flexural strength analysis. This physical anchoring confirms the ability of steel fibers to resist pull-out forces, thereby enhancing the post-cracking energy absorption capacity of the composite.

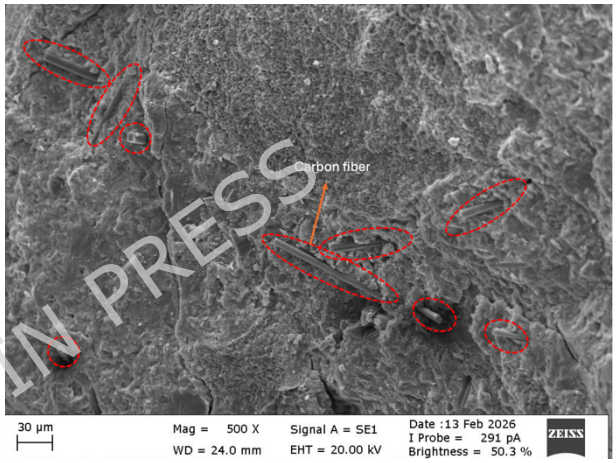
In contrast, Figure 4(b) displays the microstructure of the carbon fiber (0SF-0.30CF) reinforced specimen. The micrograph reveals that the carbon fibers, characterized by their significantly finer and high-aspect-ratio morphology, achieve a homogeneous dispersion within the matrix without noticeable agglomeration. This uniform distribution is critical for the micro-scale reinforcement effect; by occupying the interstitial spaces between hydration products, the carbon fibers act as micro-crack arresters, bridging micro-voids and delaying the coalescence of micro-cracks into macro-fractures [53].

ARTICLE IN PRESS

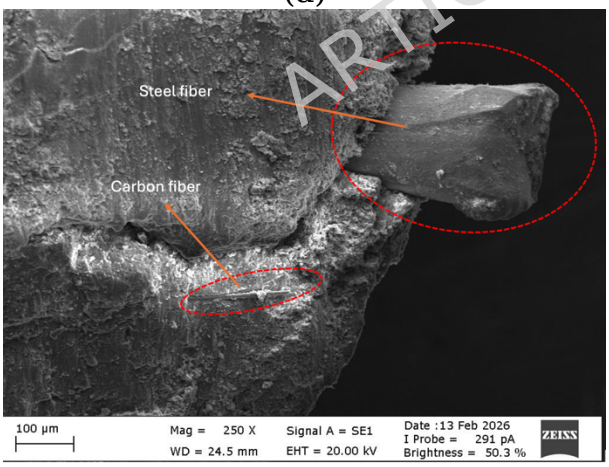
The hybrid configuration (0.50SF-0.15CF), presumably shown in the multi-scale view of Figure 4(c), demonstrates the coexistence of both macro- and micro-reinforcement phases. While the coarser steel fibers provide the primary skeletal support to arrest larger cracks, the finer carbon fibers weave through the micro-pores of the matrix, creating a continuous multi-scale reinforcement network. This visual evidence supports the synergistic trend observed in the flexural tests, where the carbon fibers stabilize the matrix at the micro-level, allowing the steel fibers to function more effectively at the macro-level. The distinct contrast between the rugged surface of the steel fibers and the slender, needle-like structure of the carbon fibers highlights the geometric complementarity of the two fiber types, which is the fundamental driver of the "synergistic peak" recorded in the 0.37SF-0.10CF specimen.



(a)



(b)



(c)

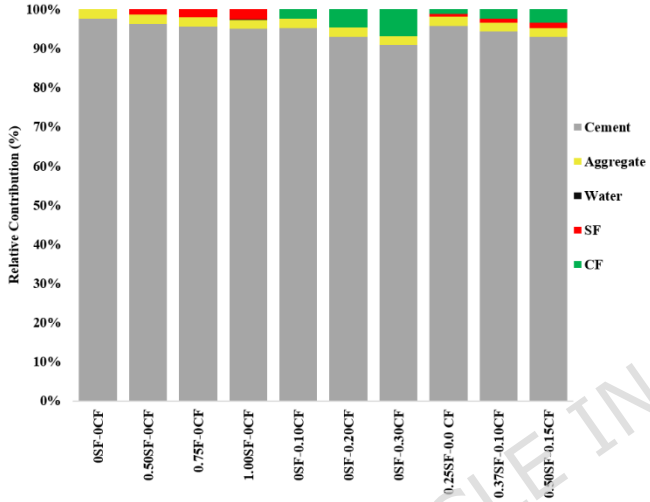
Figure 4. SEM images of (a) 1.00SF-0CF, (b) 0SF-0.30CF, and (c) 0.50SF-0.15CF specimens showing various fiber morphologies and matrix adhesion.

3.5. Life Cycle Assessment (LCA)

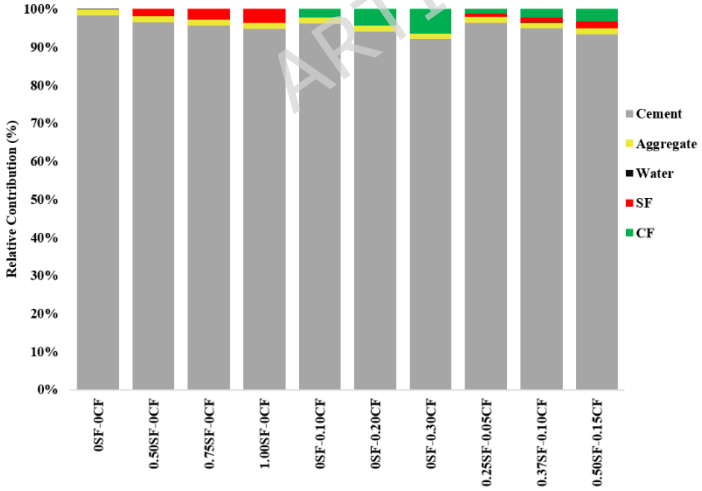
ARTICLE IN PRESS

The possible potential impacts of all the designed mortar mixes on the environment and human health are presented in Figure 5 to Figure 8. From Figure 5, it is clearly observed that the Global Warming (GW) potential is predominantly driven by the consumption of cement across all mixtures. This GW impact potential is found to be varying between 98.35% and 92.04% due to the use of cement in the mixtures. The remaining marginal percentage of GW is due to the aggregates, water, and fibers. It is a well-known fact that the manufacturing and consumption of cement in concrete is energy-intensive and hazardous to the environment due to the emission of greenhouse gases.

A. Fine Particulate Matter Formation



B. Global Warming (GW)



C. Stratospheric Ozone Depletion (SOD)

ARTICLE IN PRESS

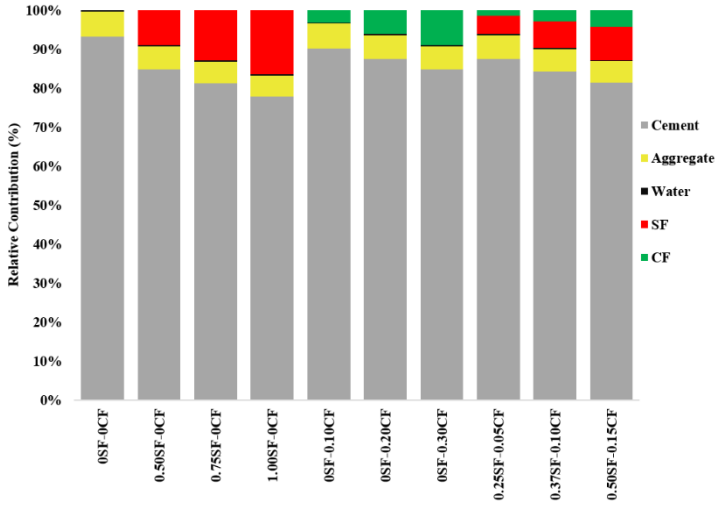
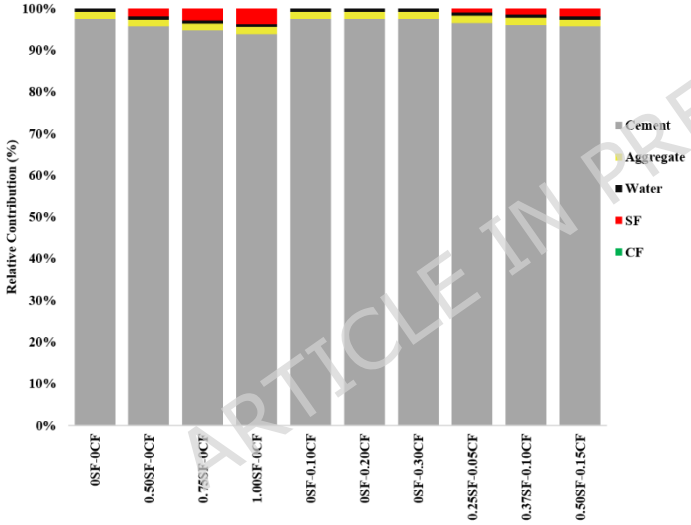


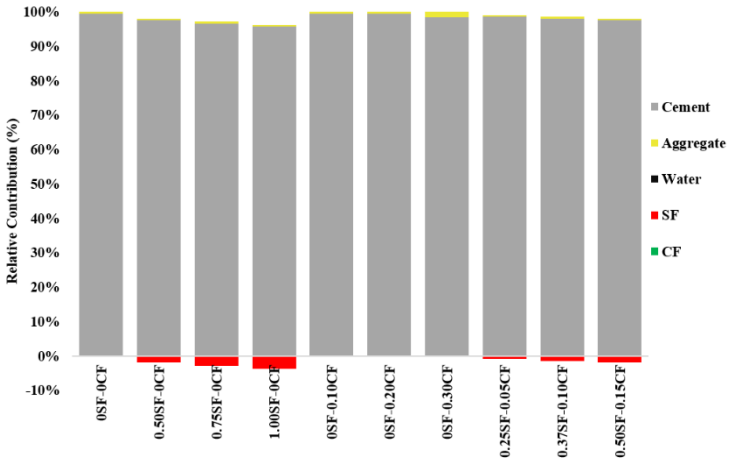
Figure 5. LCA results of the designed mixtures on A) FPMF, B) GWP, and C) SODP.

D. Marine Ecotoxicity (ME)



ARTICLE IN PRESS

E. Mineral Resource Scarcity (MRS)



ARTICLE IN PRESS

F. Fossil Resource Scarcity (FRS)

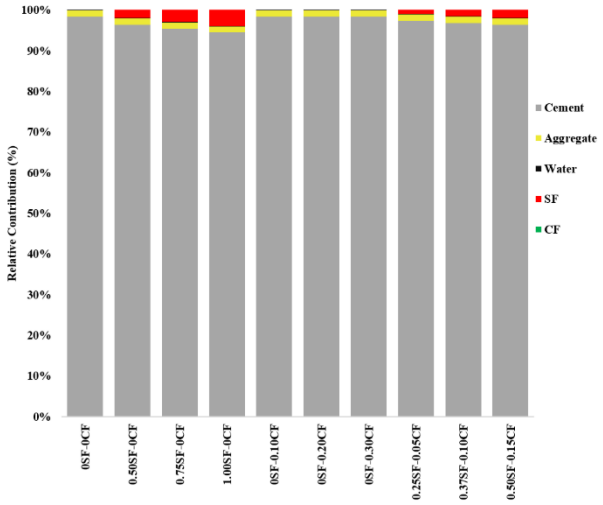
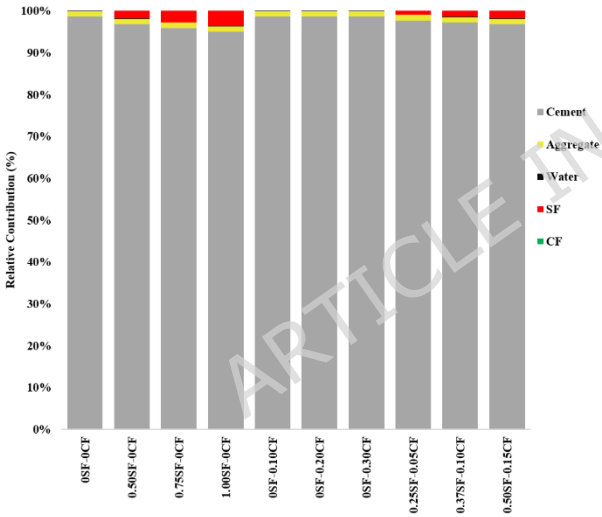


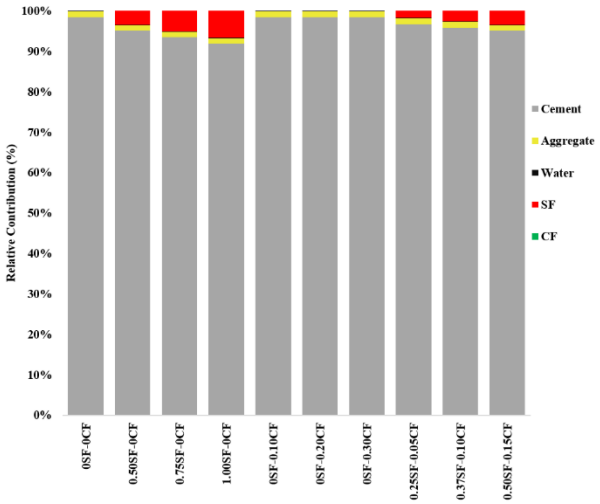
Figure 6. LCA results of the designed mixtures on D) ME, E) MRS, and F) FRS.

G. Terrestrial Ecotoxicity (TE)

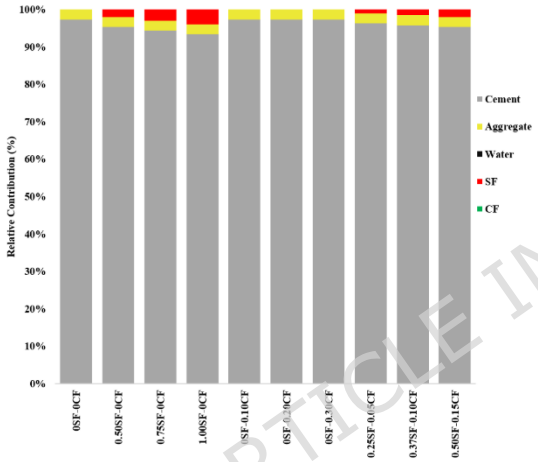


H. Human Carcinogenic Toxicity (HCT)

ARTICLE IN PRESS



I. Ozone Formation, Human Health (OFHH)

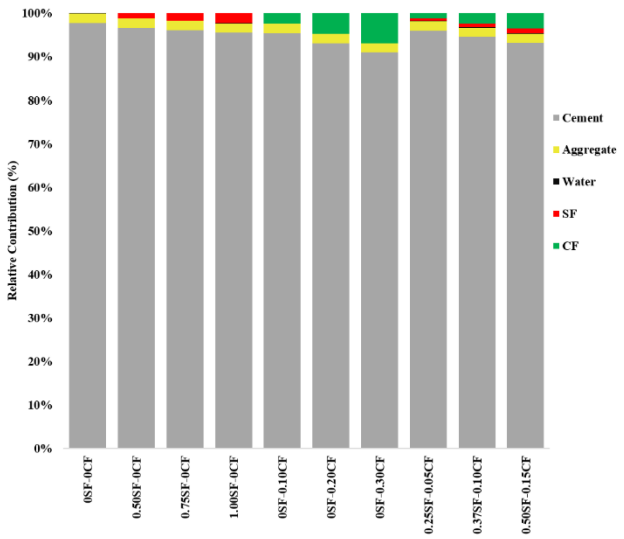


ARTICLE IN PRESS

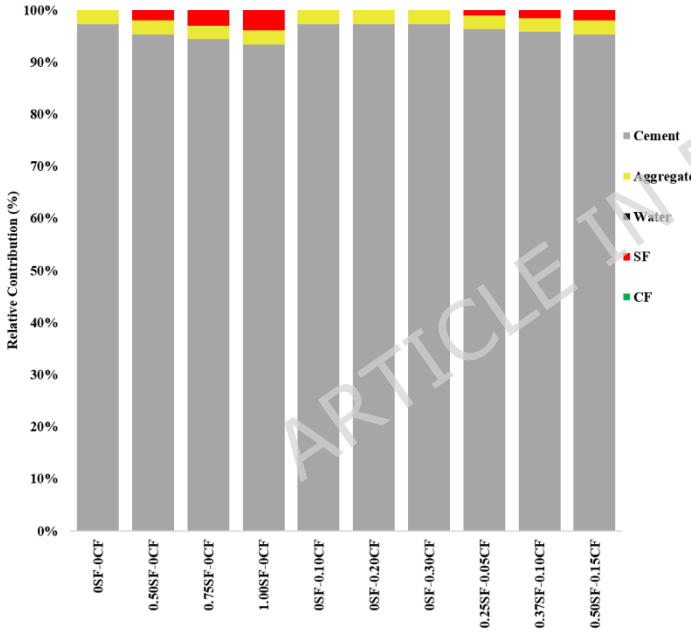
Figure 7. LCA results of the designed mixtures on G) TE, H) HCT, and I) OFHH.

J. Terrestrial Acidification (TA)

ARTICLE IN PRESS



K. Ozone Formation, Terrestrial Ecosystems (OFTE)



ARTICLE IN PRESS

Figure 8. LCA results of the designed mixtures on J) TA, and K) OFTE.

As the dosage of fibers increases, the GW impact of CF and SF reaches up to 6.41% and 3.56%, respectively, but cement remains the dominant factor. Like GW, Fine Particulate Matter Formation (FPMF) is also one of the critical impact categories, as the manufacturing and usage of concrete materials create fine particulate matter and pollute the environment. In a human health point of view, the study of FPMF is necessary, and its impact on the mixes is highlighted in Figure. 5. The impact trend of FPMF is almost identical to GW, where cement is the primary contributor, accounting for 97.57% to 90.93% of the total impact. Similarly, as the percentages of CF and SF increase, their

ARTICLE IN PRESS

impact on FPMF also increases slightly, reaching up to 6.80% and 2.63%, respectively. However, when examining Stratospheric Ozone Depletion (SOD) in Figure 5, a distinct behavior is noticed. While cement still holds the largest share (93.19% to 77.78%), the incorporation of SF exhibits a highly noticeable impact. For instance, in the 1.00SF-0CF mixture, the SOD impact of SF becomes significantly visible, contributing up to 16.54%. Similarly, the maximum SOD impact for CF is observed to be 8.98%.

An ecotoxicity is a capability that a physical or chemical compound must exhibit regarding the detrimental impact of its actions on various organisms and the environment. To evaluate these effects on marine life, Marine Ecotoxicity (ME) was analyzed, as depicted in Figure 6. The impact of the mortar mixes on the marine environment is found to be overwhelmingly dictated by the use of cement, ranging from 97.51% to 93.85%. The visual and numerical analysis indicates that the inclusion of SF shows a negligible contribution to ME (maximum 3.75%), whereas CF has almost zero impact. Furthermore, the concept of scarcity refers to the amount of minerals that can be extracted economically in the current market conditions. In this regard, Mineral Resource Scarcity (MRS) and Fossil Resource Scarcity (FRS) were also studied and are highlighted in Figure 6. In terms of MRS, cement usage exhibits the maximum mineral resource consumption. Interestingly, it is observed that the addition of SF presents a negative impact value in the MRS category, ranging from -1.00% to -4.14%. In LCA, such negative values represent an environmental credit or avoided burden. This indicates that the use of SF (which often incorporates recycled steel scrap) actually helps in conserving virgin mineral resources, thereby providing a beneficial effect against mineral depletion. However, for FRS, the energy consumption and fossil fuel depletion for cement are the highest (98.31% to 94.45%), but the manufacturing of SF also shows a visible contribution, found to be up to 3.93%. Therefore, to reduce resource consumption, alternative methods and optimized hybrid fiber designs should be followed to conserve natural resources [54].

Similarly, the impact on terrestrial environments was evaluated through Terrestrial Ecotoxicity (TE), as presented in Figure 7. Like ME, the TE impact is highly dominant for cement, varying between 98.62% and 95.07%, while SF contributes a maximum of 3.60%. The pathways to human toxicity are composed of various factors, such as environmental fate, exposure, and toxicity-effect damage. The impacts of the mixes on Human Carcinogenic Toxicity (HCT) and Ozone Formation-Human Health (OFHH) are also highlighted in Figure 7. Considering the factor of human health, the impact of HCT and OFHH is primarily governed by cement manufacturing, accounting for 98.41% to 91.87% and 97.27% to 93.39%, respectively. The secondary impact in HCT is observed for SF, which is found to be up to 6.65%.

ARTICLE IN PRESS

Furthermore, the impacts on Terrestrial Acidification (TA) and Ozone Formation in Terrestrial Ecosystems (OFTE) are presented in Figure 8. Interestingly, in the TA category, while cement is the leading cause (97.72% to 91.02%), the addition of CF exhibits a visible secondary impact, reaching up to 6.86% in high-volume mixes like 0SF-0.30CF. In the OFTE category, cement remains the major contributor (97.27% to 93.40%), with SF showing a marginal impact of up to 3.97%.

3.6. Cost Estimation Analysis

Figure 9 illustrates the material cost required to achieve 1 MPa of compressive and flexural strength (in USD/MPa). Evaluating these mixtures based solely on their initial raw material cost can be misleading; therefore, normalizing the cost against mechanical performance provides a more accurate economic assessment.

3.6.1. Cost per unit compressive strength

As shown in Figure 9, the reference plain mortar (0SF-0CF) has a unit compressive strength cost of 21.18 USD/MPa. Although the 1.00SF-0CF mixture yielded the highest absolute compressive strength, the 0.50SF-0CF mixture proved to be the most cost-effective choice, lowering the unit cost to 20.71 USD/MPa. This difference is due to a diminishing return effect: increasing the steel fiber content from 0.50% to 1.00% significantly raises the material cost but provides only a marginal strength gain (from 68.93 to 69.67 MPa), making higher fiber volumes economically inefficient for compression. Conversely, adding CF generally increased the unit cost, reaching 23.41 USD/MPa for the 0SF-0.30CF mixture. This is because carbon fibers have a higher market price and contribute less to compressive strength than steel fibers.

ARTICLE IN PRESS

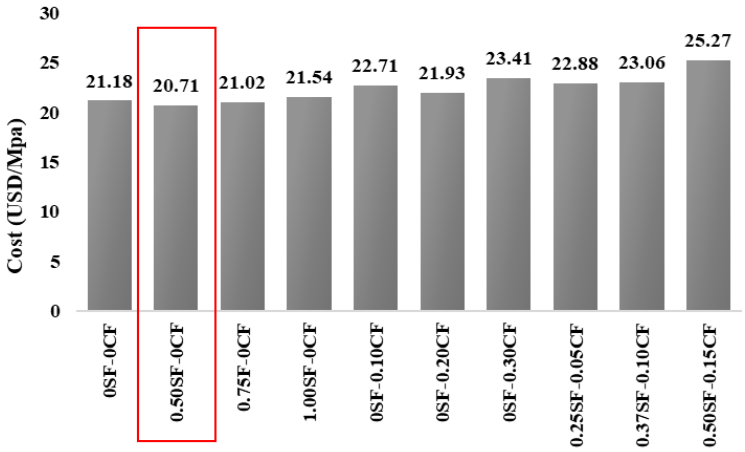


Figure 9. Cost per Unit Compressive Strength

3.6.2. Cost per unit flexural strength

ARTICLE IN PRESS

For flexural strength (Figure 10), the reference mixture exhibited the highest unit cost at 241.26 USD/MPa due to its low flexural capacity. In contrast, the 0.37SF-0.10CF hybrid mixture emerged as the most economical option, significantly reducing the unit cost to 154.88 USD/MPa. Achieving a peak flexural strength of 9.12 MPa with this mixture fully justifies the higher initial material cost of the hybrid design.

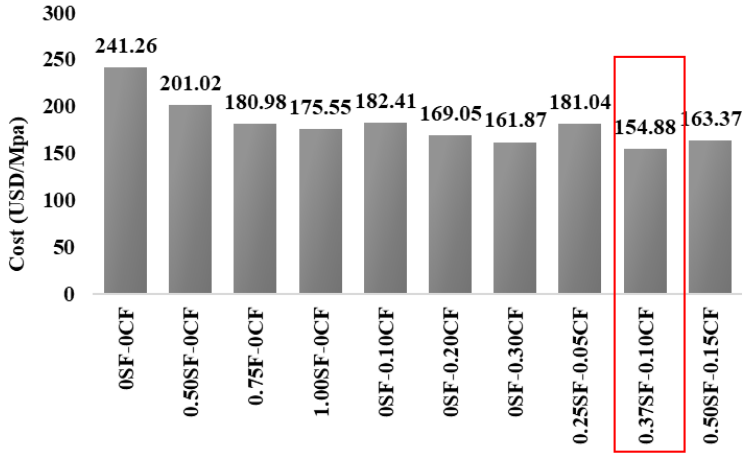


Figure 10. Cost per Unit Flexural Strength

3.7. Multi-objective performance assessment

In order to provide a more comprehensive evaluation of the developed composites, a multi-objective performance assessment is conducted by simultaneously considering mechanical performance, environmental impact, and economic efficiency. Unlike conventional approaches where these parameters are assessed independently, this study integrates them into a unified decision-making framework. Existing single-criterion metrics — such as cost per unit strength (USD/MPa) or GWP per unit strength (kg CO_2/MPa) — are valuable for isolated comparisons but do not capture simultaneous trade-offs among all three criteria. The PI proposed here integrates all three into a single efficiency index: a higher PI indicates superior mechanical performance achieved at lower combined economic and environmental cost. This formulation is conceptually aligned with eco-efficiency metrics in industrial ecology, adapted for material-level comparison of cementitious composites.

To quantify the combined performance of each mixture, a performance index (PI_{flex} and PI_{comp}) are proposed as follows:

$$PI_{flex} = f_r / (C_{total} \times GWP) \quad (3)$$

$$PI_{comp} = f_c / (C_{total} \times GWP) \quad (4)$$

where f_r is the flexural strength (MPa), f_c is the compressive strength (MPa), C_{total} is the total material cost (USD/m^3), and GWP is the global warming potential (kg CO_2-eq/m^3). This index reflects the efficiency of a mixture in delivering mechanical performance while minimizing both economic cost and environmental burden. A higher PI value indicates a more sustainable and cost-effective composite.

ARTICLE IN PRESS

Figure 11 illustrates the variation of compressive (PI_{comp})and flexural (PI_{flex}) performance indices for different fiber combinations, evaluated against total material cost (C_{total}) and global warming potential (GWP). Regarding the compressive efficiency, the control mix (0SF-0CF) maintained a PI_{comp} of $1.98x10^5$. The addition of fibers generally resulted in a downward trend in this index, with the 0.50SF-0.15CF hybrid mix exhibiting the most significant reduction of 20.37%. This decline is directly attributed to the high environmental and economic burden associated with steel and carbon fibers; the LCA data and unit costs indicate that while these reinforcements slightly enhance compressive strength, the percentage increase in the denominator ((C_{total} × GWP) is much larger than the gain in the numerator (f_c). In contrast, a significant upward trend was observed for the PI_{flex} values, where all fiber-reinforced mixtures outperformed the control mix ($0.17x10^5$). Specifically, the 0.37SF-0.10CF hybrid combination reached a peak value of $0.26x10^5$, representing a remarkable 50% increase over the reference mix. This peak indicates a superior "performance-to-impact" ratio, as the dramatic enhancement in flexural capacity (f_r) via the fiber-bridging mechanism effectively offsets the increased carbon footprint and material cost. Although the 0.37SF-0.10CF mix showed a moderate reduction in PI_{comp} of approximately 11.4%, its exceptional gain in PI_{flex} justifies its selection as the optimum design for sustainable and high-performance cementitious composites.

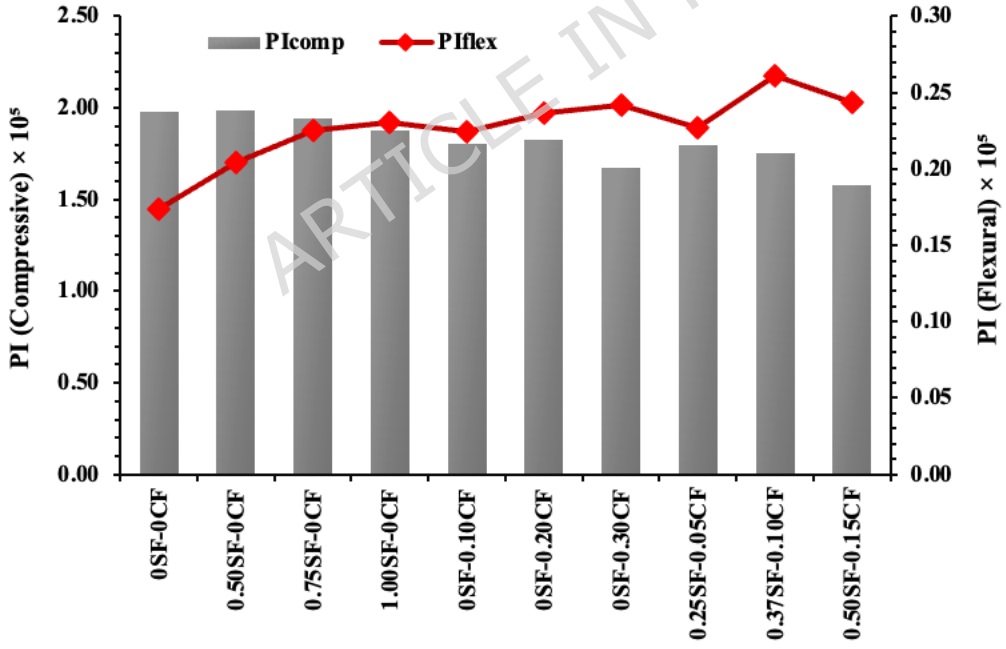


Figure 11. Variation of compressive and flexural performance indices (PI) for different fiber combinations considering cost and global warming potential.

The selection of such an optimum mixture based on conflicting criteria underscores the broader challenge of multi-criteria optimization in engineering design. The mathematical structure of the proposed PI framework serves as a deterministic alternative to complex multi-criteria

ARTICLE IN PRESS

decision-making (MCDM) methodologies frequently employed in state-of-the-art sustainability literature to resolve multi-attribute trade-offs under uncertainty. For instance, advanced scoring tools, including picture fuzzy analytical frameworks [55] and similarity-measure-based TOPSIS models [56], are widely accepted for ranking multi-criteria alternatives under strict data boundaries. Similarly, high-dimensional engineering trade-offs often rely on advanced metaheuristic search principles, such as the promoted osprey optimizer [57], to systematically validate multi-attribute technical systems. While these metaheuristic and fuzzy tools manage epistemic uncertainties or vast search spaces, the analytical PI method developed in this study translates empirical mechanical data, life-cycle costs, and emissions into a highly reproducible, direct comparative index.

4. Conclusion

This research evaluated the mechanical performance, microstructural evolution, and environmental-economic sustainability of SF-CF hybrid cementitious composites. The following key conclusions are drawn:

- **Multi-scale Synergistic Effect:** The hybrid combination of 0.37% SF and 0.10% CF yielded the highest flexural strength, demonstrating a synergistic mechanism where CF intercepts micro-cracks at early loading stages, while SF bridges macro-cracks during post-peak deformation.
- **Microstructural Refinement:** MIP and SEM analyses confirmed that the inclusion of carbon fibers effectively refines the pore structure by reducing macroporosity. CF serves as a nucleating agent for hydration products, resulting in a more homogenous and dense matrix compared to mono-steel fiber composites.
- **Threshold for Fiber Efficiency:** Excessive fiber content (beyond 0.65% total volume) leads to a decline in mechanical properties due to fiber agglomeration and increased entrapped air, which negatively impacts the matrix-fiber bond strength.
- **Environmental and Economic Viability:** Although carbon fibers have a high initial carbon footprint, their ability to enhance strength at low dosages makes hybrid systems more eco-efficient. The LCA results indicate that hybrid mixtures can reduce the GWP per MPa of flexural strength compared to conventional SF-reinforced mortars.
- **Optimization Framework:** The proposed Performance Index (PI) successfully quantifies the equilibrium between mechanical prowess, cost, and GWP. This index identifies hybrid reinforcement as a superior strategy for developing next-generation, multifunctional, and sustainable cementitious materials.
- **Long-term Durability Outlook:** The pore refinement confirmed by MIP — particularly the concentration of pores in the 10–100 nm range — is expected to contribute positively to resistance against chloride ion

ARTICLE IN PRESS

ingress and carbonation. The denser ITZ observed in SEM further supports anticipated improvements in transport properties. The presence of randomly distributed SF is known to impose internal restraint against drying shrinkage-induced cracking; however, the high surface area of CF may slightly increase early-age autogenous shrinkage at higher dosages. Future research should systematically evaluate drying shrinkage, accelerated carbonation resistance, and chloride diffusion coefficients of the optimized hybrid mixture.

Data Availability Statement

All data generated or analysed during this study are included in this article.

Competing interests

The authors declare that they have no competing interests.

Acknowledgments

The author would like to express his sincere thanks to Hamit Tavan for his valuable assistance during the experimental studies.

Funding: This study was supported by Bursa Uludag University Research Projects Coordination Office under the Grant Number FGA-2025-2027. The authors thank to BUU BAP Unit for their support.

ARTICLE IN PRESS

Reference

1. Adesina, A. & Zhang, J. Impact of concrete structures durability on its sustainability and climate resiliency. *Next Sustainability* **3**, 100025 (2024).
2. Qureshi, H. J. *et al.* Investigation of CFRP Reinforcement Ratio on the Flexural Capacity and Failure Mode of Plain Concrete Prisms. *Materials* **15**, (2022).
3. Chahar, A. S. & Pal, P. Study on various properties of reinforced concrete – A review. *Materials Today: Proceedings* **65**, 597–602 (2022).

ARTICLE IN PRESS

4. Hassan, H. Z. & Saeed, N. M. Fiber reinforced concrete: a state of the art. *Discov Mater* **4**, 101 (2024).

5. Anas, M., Khan, M., Bilal, H., Jadoon, S. & Khan, M. N. Fiber Reinforced Concrete: A Review. *Engineering Proceedings* **22**, (2022).

6. El-Abbasy, A. A. Tensile, flexural, impact strength, and fracture properties of ultra-high-performance fiber-reinforced concrete – A comprehensive review. *Construction and Building Materials* **408**, 133621 (2023).

7. Devaraj, R., Olofinjana, A. & Gerber, C. Making a Case for Hybrid GFRP-Steel Reinforcement System in Concrete Beams: An Overview. *Applied Sciences* **13**, (2023).

8. Rabi, M., Shamass, R. & Cashell, K. A. Structural performance of stainless steel reinforced concrete members: A review. *Construction and Building Materials* **325**, 126673 (2022).

9. Amirtharaj, J. & Rose, A. L. A state-of-the-art review on the structural behavior of concrete structures reinforced with various rebars as alternative to steel rebars. *Journal of Building Engineering* **111**, 113387 (2025).

10. Niu, Y., Wei, J. & Jiao, C. Multi-scale fiber bridging constitutive law based on meso-mechanics of ultra high-performance concrete under cyclic loading. *Construction and Building Materials* **354**, 129065 (2022).

11. Gribniak, V. & Sokolov, A. Standardized RC beam tests for modeling the fiber bridging effect in SFRC. *Construction and Building Materials* **370**, 130652 (2023).

ARTICLE IN PRESS

ARTICLE IN PRESS

12. Ali, A. Y. F., El-Emam, H. M., Seleem, M. H., Sallam, H. E. M. & Moawad, M. Effect of crack and fiber length on mode I fracture toughness of matrix-cracked FRC beams. *Construction and Building Materials* **341**, 127924 (2022).

13. Zhou, W.-D., Zhang, D.-M., Zhang, X., Huang, Z.-K. & Xie, X.-C. Experimental and mesoscale numerical investigation on tensile properties of steel fibre-reinforced concrete. *Construction and Building Materials* **458**, 139601 (2025).

14. Akbulut, Z. F., Tawfik, T. A., Smarzewski, P. & Guler, S. Advancing Hybrid Fiber-Reinforced Concrete: Performance, Crack Resistance Mechanism, and Future Innovations. *Buildings* **15**, (2025).

15. Accornero, F., Rubino, A. & Carpinteri, A. Post-cracking regimes in the flexural behaviour of fibre-reinforced concrete beams. *International Journal of Solids and Structures* **248**, 111637 (2022).

16. Ding, Y., Guo, W., Li, D. & Pacheco-Torgal, F. Exploring the effect of polyoxymethylene fiber on concrete toughness and self-sensing capability of concrete cracking under bending. *Construction and Building Materials* **454**, 138933 (2024).

17. Savio, A. A. D., Esquivel, D. L. T. & Landeo, J. M. G. Post-Cracking Properties of Concrete Reinforced with Polypropylene Fibers through the Barcelona Test. *Polymers* **15**, (2023).

ARTICLE IN PRESS

ARTICLE IN PRESS

18. Akgol, O. *et al.* A Nondestructive Method for Determining Fiber Content and Fiber Ratio in Concretes Using a Metamaterial Sensor Based on a V-Shaped Resonator. *J. Electron. Mater.* **48**, 2469–2481 (2019).

19. Aksoy, A., Yigit, E., Caglayan, A. B. & Ozturk, M. Interpretation and analysis of scattering in steel fiber alignment in concrete: The H alpha decomposition method using fully polarized B-scan ground penetrating radar (GPR) image data. *Journal of Building Engineering* **105**, 112472 (2025).

20. Ozturk, M., Sevim, U. K., Akgol, O., Karaaslan, M. & Unal, E. An electromagnetic non-destructive approach to determine dispersion and orientation of fiber reinforced concretes. *Measurement* **138**, 356–367 (2019).

21. Clarke, T., Ghiji, M., Fragomeni, S. & Guerrieri, M. Mechanical properties of macro synthetic fiber reinforced concrete at elevated temperatures: A systematic review and meta-analysis. *Structural Concrete* **24**, 1244–1270 (2023).

22. de Assis, H. J. B., da Silva Bezerra, A. C., de Paula, J. N. & Moravia, W. G. Utilization of recycled synthetic fibers in concrete with a focus on structural properties enhancement: a critical literature review. *Discov Mater* **4**, 77 (2024).

23. Sadrinejad, I., Madandoust, R. & Ranjbar, M. M. The mechanical and durability properties of concrete containing hybrid synthetic fibers. *Construction and Building Materials* **178**, 72–82 (2018).

ARTICLE IN PRESS

ARTICLE IN PRESS

24. Prakash Chandar, S. & Sangeeth Kumar, S. K. Mechanical properties of fiber reinforced concrete – natural fibers: A review. *Materials Today: Proceedings* **68**, 2066–2071 (2022).

25. Jahami, A., Zeaiter, N. & Cheaib, M. Reviewing the potential: a comprehensive review of natural fibers (NFs) in structural concrete and their multifaceted influences. *Innov. Infrastruct. Solut.* **9**, 102 (2024).

26. Elsayed, M., Abd-Allah, S. R., Said, M. & El-Azim, A. A. Structural performance of recycled coarse aggregate concrete beams containing waste glass powder and waste aluminum fibers. *Case Studies in Construction Materials* **18**, e01751 (2023).

27. Dominguez-Santos, D., Pallarés, F. J. & Llanos, P. Seismic structural performance of concrete blocks with steel and aluminum alloy fiber aggregates for building construction. *Mechanics of Advanced Materials and Structures* **29**, 6907–6918 (2022).

28. Abbass, W., Khan, M. I. & Mourad, S. Evaluation of mechanical properties of steel fiber reinforced concrete with different strengths of concrete. *Construction and Building Materials* **168**, 556–569 (2018).

29. Zhang, R., Yan, X. & Guo, L. Pullout damage analysis of steel fiber with various inclination angles and interface states in UHPC through acoustic emission and microscopic observation. *Journal of Building Engineering* **51**, 104271 (2022).

ARTICLE IN PRESS

ARTICLE IN PRESS

30. Sayam, A. *et al.* A review on carbon fiber-reinforced hierarchical composites: mechanical performance, manufacturing process, structural applications and allied challenges. *Carbon Lett.* **32**, 1173–1205 (2022).

31. Das, T. K., Ghosh, P. & Das, N. Ch. Preparation, development, outcomes, and application versatility of carbon fiber-based polymer composites: a review. *Adv Compos Hybrid Mater* **2**, 214–233 (2019).

32. Das, T. K., Jesionek, M., Ali, M. D., Ganguly, S. & Poater, A. Advancing sustainability: circular economy strategies for fibrous polymer composites. *Cleaner Materials* **19**, 100381 (2026).

33. Das, T. K. & Jesionek, M. Synthesis, Properties, and Characterization of Fibrous Filler. in *Fiber and Ceramic Filler-Based Polymer Composites for Biomedical Engineering* (eds Parameswaranpillai, J., Ganguly, S., Das, P. & Gopi, J. A.) 63–85 (Springer Nature, Singapore, 2024). doi:10.1007/978-981-97-3909-7_4.

34. Zia, A., Zhang, P. & Holly, I. Long-term performance of concrete reinforced with scrap tire steel fibers in hybrid and non-hybrid forms: Experimental behavior and practical applications. *Construction and Building Materials* **409**, 134011 (2023).

35. Xia, L. *et al.* Synergistic effect of hybrid micro- and macro- fibers on the flexural properties of concrete. *Construction and Building Materials* **462**, 139901 (2025).

ARTICLE IN PRESS

ARTICLE IN PRESS

36. Alshannag, M., Alshmalani, M., Alsaif, A. & Higazey, M. Flexural performance of high-strength lightweight concrete beams made with hybrid fibers. *Case Studies in Construction Materials* **18**, e01861 (2023).

37. Liu, X., Chen, Z., Zhang, Y., Chen, P. & Zhang, Y. Mechanical properties and flexural toughness evaluation method of mono/hybrid fiber-reinforced ultra-high performance seawater sea sand concrete. *Construction and Building Materials* **461**, 139861 (2025).

38. Park, J.-G., Seo, D.-J. & Heo, G.-H. Impact Resistance and Flexural Performance Properties of Hybrid Fiber-Reinforced Cement Mortar Containing Steel and Carbon Fibers. *Applied Sciences* **12**, (2022).

39. Niu, Y., Wei, J. & Jiao, C. Crack propagation behavior of ultra-high-performance concrete (UHPC) reinforced with hybrid steel fibers under flexural loading. *Construction and Building Materials* **294**, 123510 (2021).

40. Rutzen, M. *et al.* Influence of fiber alignment on pseudoductility and microcracking in a cementitious carbon fiber composite material. *Mater Struct* **54**, 58 (2021).

41. Lim, D. & Choi, M. Methodology for analyzing the bond failure behavior of carbon fiber-reinforced polymer reinforced structures based on stress field theory. *Journal of Building Engineering* **108**, 112923 (2025).

42. Zhang, J. & Li, V. C. Simulation of crack propagation in fiber-reinforced concrete by fracture mechanics. *Cement and Concrete Research* **34**, 333–339 (2004).

ARTICLE IN PRESS

ARTICLE IN PRESS

43. Xia, L. *et al.* Synergistic effect of hybrid micro- and macro- fibers on the flexural properties of concrete. *Construction and Building Materials* **462**, 139901 (2025).

44. Mizani, J., Sadeghi, A. M. & Afshin, H. Experimental study on the effect of macro and microfibers on the mechanical properties of reactive powder concrete. *Structural Concrete* **23**, 240–254 (2022).

45. Li, K. F. *et al.* Effects of hybrid fibers on workability, mechanical, and time-dependent properties of high strength fiber-reinforced self-consolidating concrete. *Construction and Building Materials* **277**, 122325 (2021).

46. Li, Y., Zhao, C., Li, H. & Liu, W. Study on the toughness and microstructure of UHPC with a high steel fiber content. *Construction and Building Materials* **460**, 139810 (2025).

47. Park, S.-J., Seo, M.-K., Shim, H.-B. & Rhee, K.-Y. Effect of different cross-section types on mechanical properties of carbon fibers-reinforced cement composites. *Materials Science and Engineering: A* **366**, 348–355 (2004).

48. González, D. C., Rahman, M., Mínguez, J., Vicente, M. A. & Hindi, R. Influence of Fibers and Curing Conditions on the Pore Morphology in Plain and Fiber-Reinforced High-Performance Concrete through the Use of Computed Tomography Scan Technology. *Applied Sciences* **10**, (2020).

49. Huang, D., Wang, X., Li, X., Su, L. & Tian, J. Advanced nuclear magnetic resonance technology analysis of hybrid fiber reinforced concrete for

ARTICLE IN PRESS

ARTICLE IN PRESS

optimized pore structure and strength. *Construction and Building Materials* **467**, 140383 (2025).

50. Huang, H. *et al.* Micromechanical properties of interfacial transition zone between carbon fibers and UHPC matrix based on nano-scratching tests. *Cement and Concrete Composites* **139**, 105014 (2023).
51. Zhao, Y., Xiang, J., Qiang, S. & Lu, H. Study on the optimization of electromechanical properties and fiber dispersion mechanisms in red mud-carbon fiber-cement ternary composites. *Construction and Building Materials* **490**, 142527 (2025).
52. Yuan, Q. *et al.* Interfacial bonding properties of novel strand steel fiber and cement matrix: Experimental and analytical investigations. *Construction and Building Materials* **472**, 140835 (2025).
53. Ozturk, M. Effect of recycling methods on microstructure and mechanical properties of carbon fiber cementitious composite. *Journal of Adhesion Science and Technology* **39**, 2903–2920 (2025).
54. Dharek, M. S., M, M., S, B., Vengala, J. & Tangadagi, R. B. Performance evaluation of hybrid fiber reinforced concrete on engineering properties and life cycle assessment: A sustainable approach. Journal of Cleaner Production 458, 142498 (2024).
55. V. Govindarajan, S. Shahab, A. Yousef, Z. A. Shaikh, A. K. Dutta, M. Anjum, "A picture fuzzy multi-criteria decision-making framework for evaluating urban planning proposals under uncertainty," Ain Shams Engineering Journal, vol. 17, p. 104098, 2026.

ARTICLE IN PRESS

ARTICLE IN PRESS

56. V. Govindarajan, A. Yousef, A. I. Chaudhary, A. Ahmad, Z. A. Shaikh, "A Similarity Measures-Based TOPSIS Method for Neutrosophic Hypersoft Set with Application in Crop Production," Engineering, Technology & Applied Science Research, vol. 16, no. 1, pp. 31863-31873, 2026.

57. Z. Liu, X. Jian, T. Sadiq, Z. A. Shaikh, O. Alfarraj, F. Alblehai, A. Tolba, "Promoted Osprey Optimizer: a solution for ORPD problem with electric vehicle penetration," Scientific Reports, vol. 14, Art. no. 28052, 2024.

ARTICLE IN PRESS